Applied Surface Science 256 (2010) 2414–2418

Contents lists available at ScienceDirect

Applied Surface Science

journal homepage: www.elsevier.com/locate/apsusc

The effect of back electrode on the formation of electrodeposited CoNiFe magnetic nanotubes and nanowires

F.E. Atalay [a,*], H. Kaya [a], V. Yagmur [a], S. Tari [b], S. Atalay [a], D. Avsar [a]

[a] Inonu University, Science and Art Faculty, Department of Physics, Malatya 44280, Turkey
[b] IYTE, Science Faculty, Department of Physics, İzmir, Turkey

ARTICLE INFO

Article history:
Received 22 May 2009
Accepted 22 October 2009
Available online 31 October 2009

PACS:
62.23.Hj
61.46.Np
81.07.−b
81.15.Pq
75.50.Bb

Keywords:
CoNiFe nanowires
CoNiFe nanotubes
Electrodeposition
Magnetic properties
Back electrode

ABSTRACT

The electrodeposition of cobalt + nickel + iron alloy nanostructures in aqueous sulfate solution has been studied using vitreous templates placed on highly ordered porous anodic alumina oxide (AAO). During the deposition process some electrochemical bath parameters such as ion content, deposition voltage, pH and temperature of solution were kept constant. The morphological properties of the nanostructures were studied by scanning electron microscopy (SEM) and the chemical composition was determined by examination of the energy dispersive X-ray (EDX) spectra. The magnetic behaviour of the arrays was determined with a vibrating sample magnetometer (VSM). Voltammetric and galvanostatic results indicate that the back electrodes placed on AAO plays the main role in obtaining nanowire or nanotube structured material.

1. Introduction

Recently, a number of methods have been developed to fabricate one-dimensional or linear nanostructures, namely, nanotubes and nanowires. In the electronic sector, nanowires and nanotubes are attractive nanostructured materials for electronic, optoelectronic, and sensor applications because of their unique properties [1–7]. Nanostructured materials offer an incomparable opportunity to simultaneously optimize traditionally contradictory material properties. The incomparable physical properties of nanowires and nanotubes create from either the small dimensions of the objects, or structural modifications induced by the confined synthesis and surface effects. These properties make them very promising for applications in nanoelectronics and nanosensors in particular [8]. Their magnetic, electrical, mechanical and optical properties differ from their bulk counterparts.

To date, there have been a number of reports on the fabrication, structure and magnetic properties of binary or ternary systems composed entirely of pure ferromagnetic elements, e.g. NiFe, CoFe, CoNiFe, etc. [9–20]. Ferromagnetic metal alloy nanowires have received considerable attention due to applications in the area of ultra-high density magnetic recording and promising giant-magnetoresistance (GMR) properties [21].

Electrodeposition is the best method for producing magnetic nanowires. In addition to cheapness, electrodeposition is one of the few methods that can deal with the geometrical restrictions of inserting metals into very deep nanometric indentation, making it the preferred method for nanowire and nanotube production. In the electrodeposition process, the shape and dimensions of the as-deposited 1D materials can be easily controlled by selection of the geometric structures of the template used as the cathode. Up till now, studies of the growth mechanism of nanowires or nanotubes have been concerned with the nature of the material and the chemistry of the pore wall [22–25]. However, the effect of back electrode on the formation of electrodeposited CoNiFe magnetic nanotubes and nanowires has not been reported. In this work, CoNiFe nanowires and nanotubes have been fabricated using electrodeposition in structured nanoporous Al_2O_3 using different templates.

2. Experimental details

A three-electrode cell was used for the electrochemical experiments. The volume of the electrochemical bath was approximately 85 ml. An Ag/AgCl electrode (BAS, 3 M NaCl, and

* Corresponding author. Tel.: +90 4223410010; fax: +90 4223410037.
E-mail address: fatalay@inonu.edu.tr (F.E. Atalay).

0169-4332/$ – see front matter © 2009 Elsevier B.V. All rights reserved.
doi:10.1016/j.apsusc.2009.10.077

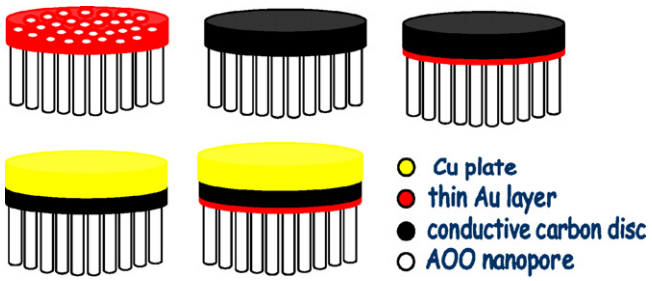

Fig. 1. Schematic diagram for different back contacts.

−35 mV versus SCE at 25 °C) was used as the reference electrode. Anodic alumina oxide (AAO) membranes, with specified pore diameters of 200 nm and pore length of 60 μm, were used as a cathode with an exposed area of approximately 1 cm^2 for the nanowire and nanotube synthesis. These membranes were supplied by the Whatman Company. Before the electrodeposition, one side of the AAO templates was coated with Au to a thickness of 5–10 nm or had a conductive carbon disc or carbon disc on copper plate stuck on for electrical contact. Schematic diagram for different back contacts is given in Fig. 1. Insulation of back electrode from the bulk electrolyte was made by the insulation tape stuck on the conducting backside of the working electrode. A platinum electrode approximately 5 times larger than the cathode was used as an auxiliary electrode. The bath contents are given in Table 1. All solutions were prepared by dissolving reagent-grade chemicals in distilled water. The bath pH was adjusted to 2.6 by adding 0.1 mM HCl or 0.1 mM NaOH while monitoring with a Jenway 3520 pH meter. The deposition was performed at −2 V for 180 min to produce nanowires. The electrodeposition was controlled by a computer-controlled electrochemical workstation made in-house [26]. Cyclic voltammetry (CV) for the electroplating of CoNiFe was performed by means of an electrochemical analyzer system, Iviumstat potentiostat/galvanostat. The scan rate for CV was kept at 25 mV s^{-1}.

The morphology of the nanoarrays was investigated by scanning electron microscopy (SEM; LEO-EVO-40 instrument).

Table 1
Bath contents and electrodeposition conditions for production of CoNiFe nanostructures.

Chemicals	Concentration
$Co(SO_4)_2{\cdot}6H_2O$	5 mM
$Ni(SO_4)_2{\cdot}6H_2O$	200 mM
$Fe(SO_4)_2{\cdot}7H_2O$	10 mM
H_3BO_3	0.2 M
NaCl	35 mM
Sodium lauryl sulfate	0.1 g/l
Operating conditions	
Bath pH 2.6	
Bath temperature = room temperature	
Deposition duration = 180 min	
Deposition potential = −2 V versus Ag/AgCl	
Agitation paddle (5 cycles/s)	

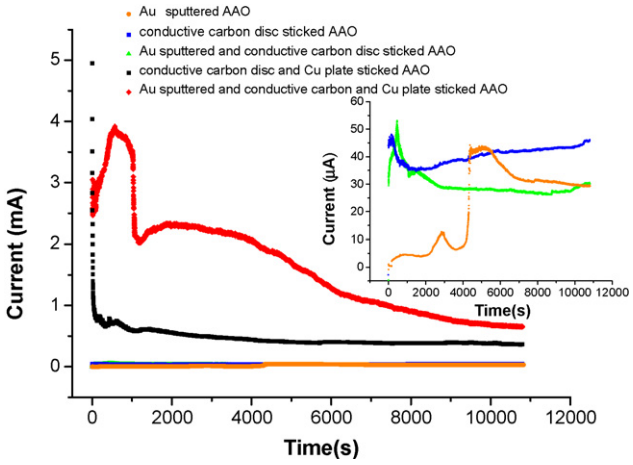

Fig. 3. Current transient curve of CoNiFe electrodeposition solution at −2 V constant deposition potential for 180 min versus Ag/AgCl. Inset shows low current region.

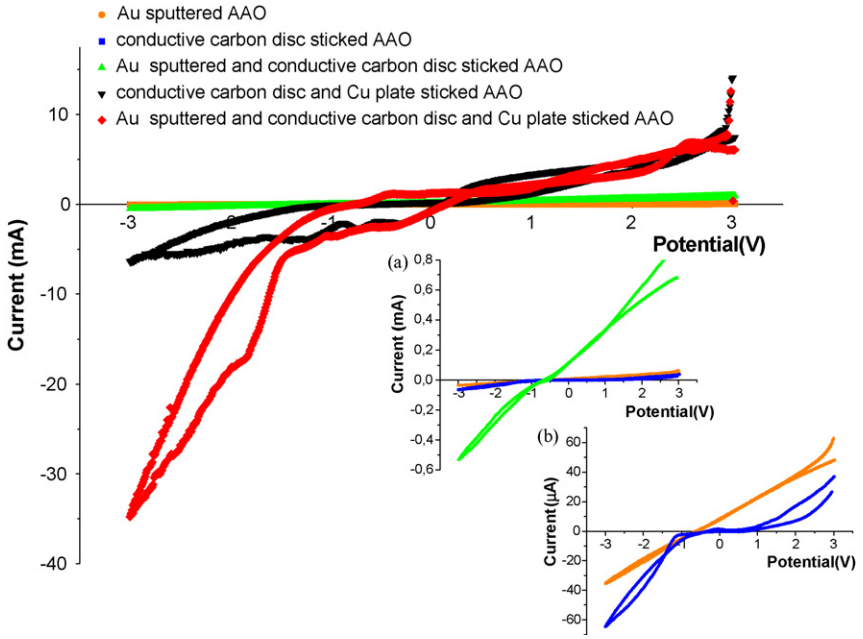

Fig. 2. Cyclic voltammograms of Co–Ni–Fe at 25 mV/s from solution of 5 mM $Co(SO_4)_2{\cdot}6H_2O$, 10 mM $Fe(SO_4)_2{\cdot}6H_2O$, 0.2 M $Ni(SO_4)_2{\cdot}6H_2O$, 35 mM NaCl, 0.01 g/l $C_{12}H_{25}NaO_4S$ on different templates. The insets are the cyclic voltammograms of Co–Ni–Fe: (a) in mA range and (b) in μA range.

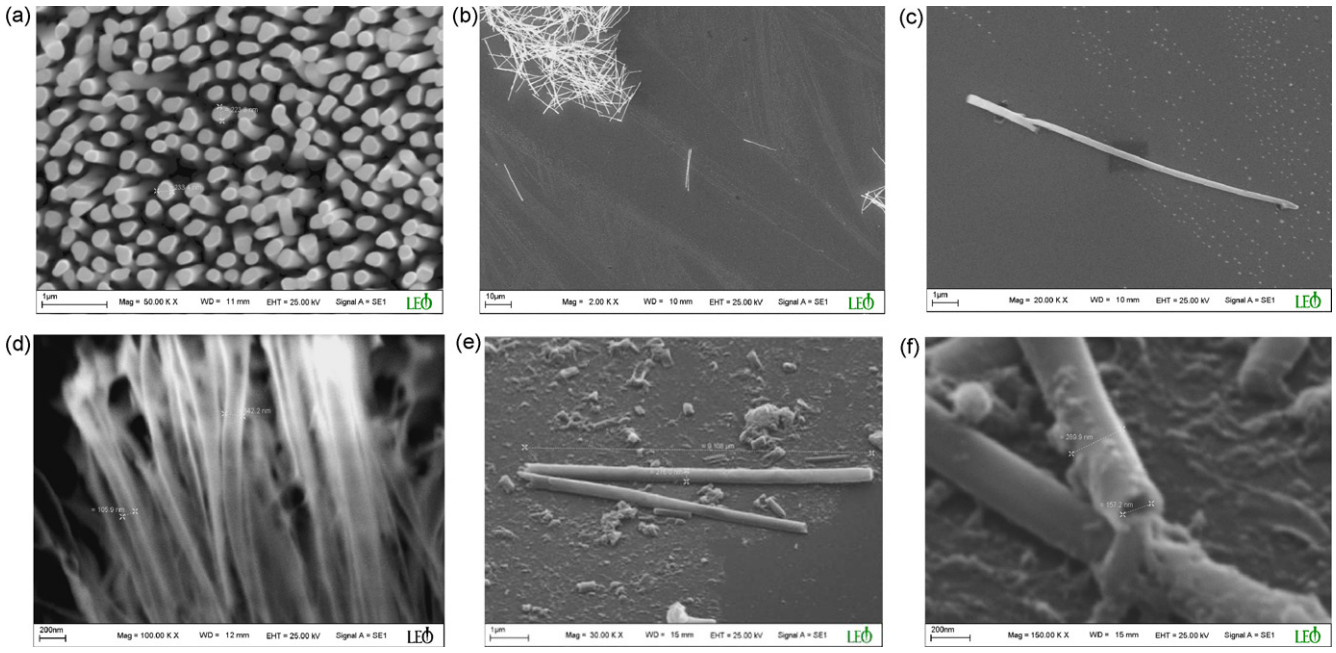

Fig. 4. (a) SEM images of ordered CoNiFe nanowire arrays electrodeposited at pH 2.6 after etching in 1 M NaOH for 5 min. (b and c) single CoNiFe nanotube after etching in 1 M NaOH for 1 h. (d) SEM images of ordered CoNiFe nanotube arrays electrodeposited at pH 2.6 after etching in 1 M NaOH for 5 min. (e and f) two CoNiFe nanotubes after etching in 1 M NaOH for 1 h. Deposition time is 180 min.

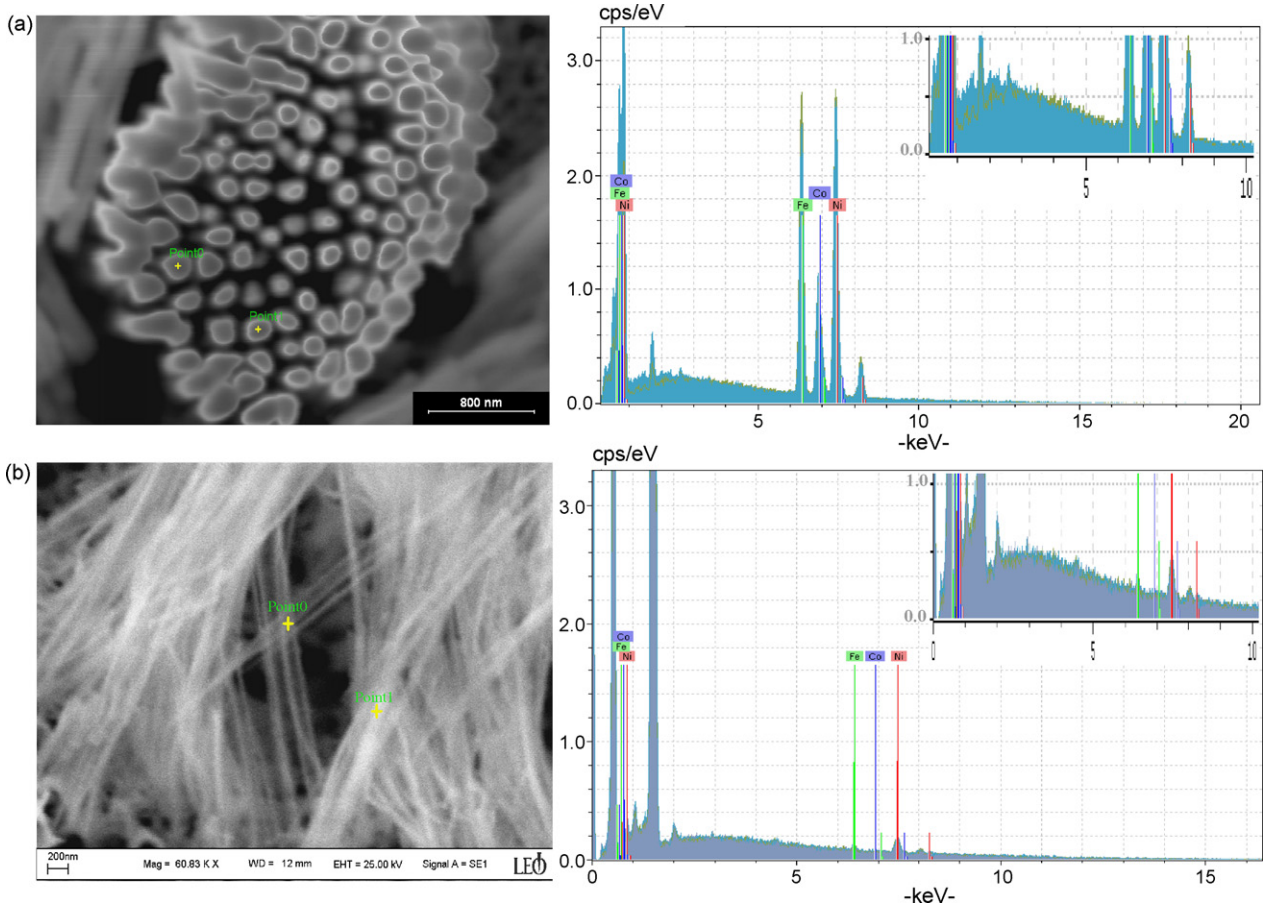

Fig. 5. EDX point analysis results: (a) $Co_{16}Ni_{57}Fe_{27}$ nanowire bundle and (b) $Co_{19}Ni_{57}Fe_{23}$ nanotube array. Insets show magnified EDX micrographs.

The quantitative chemical analyses of the alloys were performed by energy dispersive X-ray (EDX) spectroscopy. Magnetic measurements of the arrays as a whole were performed with a vibrating sample magnetometer (VSM; Lake Shore 7407).

3. Results and discussions

Typical cyclic voltammograms for CV plating of CoNiFe deposition for vitreous template electrodes are shown in Fig. 2. The CV curves generally show that there are three reaction regions corresponding to cathodic deposition, no reaction and anodic oxidation processes. On both the positive and negative sweeps of all curves except the Au sputtered template, cathodic currents are clearly found, indicating that nickel, cobalt and iron ions can be deposited into the AAO templates. Also, anodic currents are found that can be attributed to the dissolution of already-deposited metal atoms. The cyclic voltammograms of identical electrolytes containing Fe, Ni, Co at 25 mV s^{-1} indicated that the reduction of CoNiFe begins above −0.32 V, −0.66 V, −0.74 V, −0.75 V for conductive carbon disc stuck on to the AAO, Au sputtered AAO with stuck conducting carbon disc, conductive carbon disc and Cu plate stuck on to the AAO, Au sputtered AAO with stuck conducting carbon disc and Cu plate, respectively.

Fig. 3 shows the effect of the back electrode on the time dependence of the cathodic current during the CoNiFe alloy nanostructure deposition into AAO. Electrodeposition curves were obtained in a stirred electrolyte at a constant potential of −2 V versus Ag/AgCl. The current versus time plot shows that growth of the nanostructures was often not a steady-state process, and it appears that there was significant current oscillation as the voltage was applied to the cathode. There are no reduction peaks for Au sputtered AAO in Fig. 2, but a plating current (∼30–40 μA) has been observed. This must be the deposition of a thin metal layer on pore walls. A ∼2–3 mA plating current for the Au sputtered AAO with stuck conducting carbon disc and Cu plate was also observed, as shown in Fig. 3. The current increased suddenly when the pores were empty, and dropped gradually until the pores were entirely filled. As already reported [27–31], at the first stage of the current–time transient curve (Fig. 3), the porous deposition is believed to be due to the side reactions occurring in the metal deposition. Firstly, hydrogen from the side reactions may be included in the deposit. Secondly, metal hydroxide can precipitate at a high pH resulting from the side reactions. This 'crispy' part of the deposit is weak and cannot be sustained during electrodeposition. This effect is apparently reflected by a fluctuation in the current transient curves in the first 10 min. However, this period is too long for the Au sputtered AAO (∼75 min).

The general morphology of the electrodeposited CoNiFe alloys inside the pores of the AAO was studied by scanning electron microscopy (SEM). SEM images of nanowires are shown in Fig. 4a

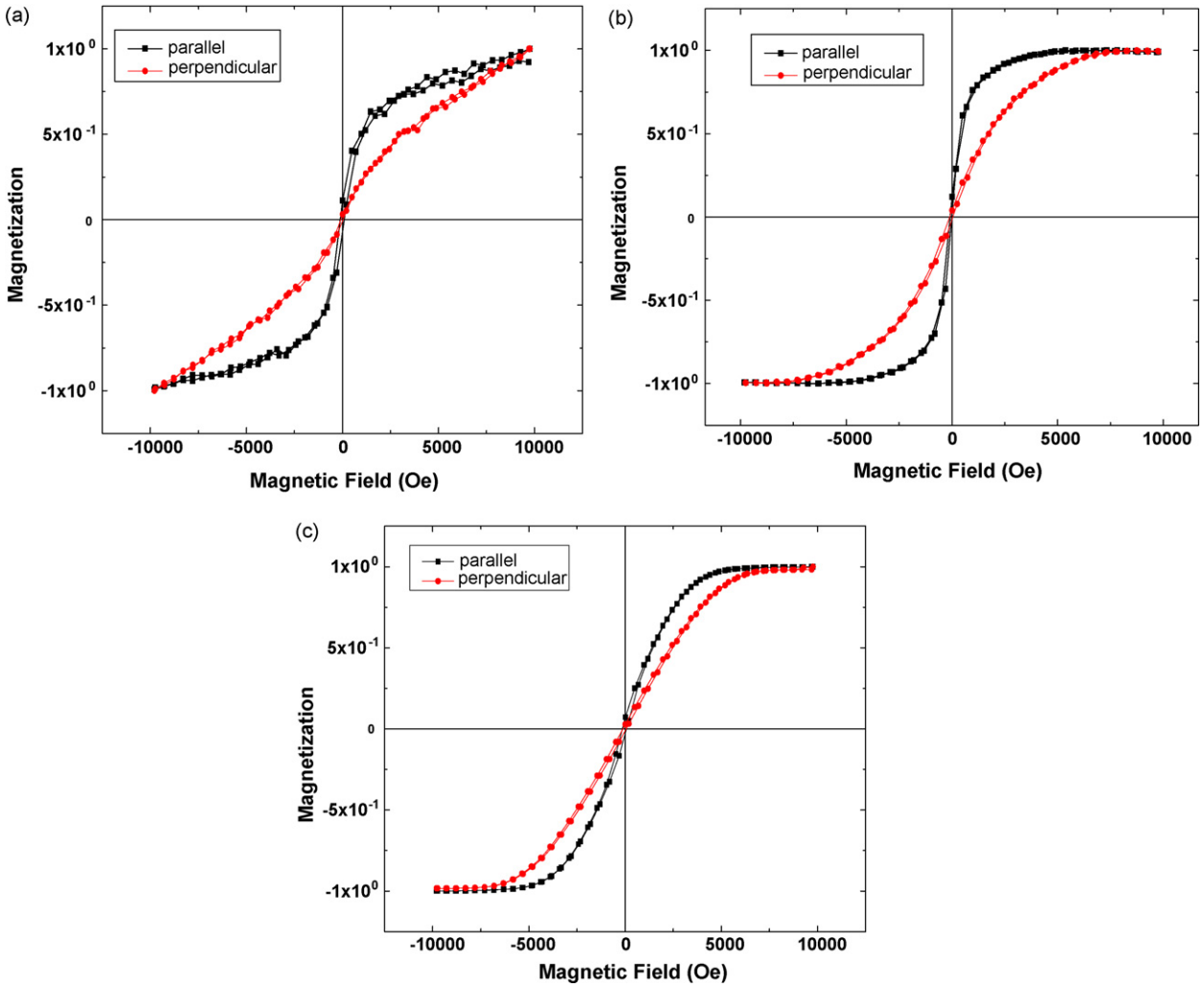

Fig. 6. *M–H* loops of: (a) CoNiFe nanotube arrays on Au sputtered AAO, (b) CoNiFe nanotube arrays on Au sputtered AAO with stuck conducting carbon disc, (c) CoNiFe nanowire arrays on Au sputtered AAO with stuck Cu plate and conducting carbon disc. Magnetic field is applied (■) parallel ((●) perpendicular) to nanotube or nanowire length.

after etching in 1 M NaOH for 5 min and in Fig. 4b and c after removing completely. We can see from the figures that the diameter and length of the well-aligned nanowires are about 200 nm and 10 μm. These nanowires are obtained using the Au sputtered AAO with stuck conducting carbon disc and Cu plate. In Fig. 4d–f, SEM images of ordered CoNiFe nanotube arrays produced using the Au sputtered AAO template are given. Typically, the lengths of the tubes are about 9 μm, with outer diameters about 250 nm and inner diameters about 150 nm.

The average composition of the CoNiFe alloy nanowires and nanotubes was evaluated by EDX microanalysis as shown in Fig. 5. This makes it clear that, apart from signals from the constituent elements nickel and iron, there are stronger signals from aluminum and oxygen from the AAO template. The CoNiFe nanowire sample electrodeposited on the Au sputtered AAO with stuck conducting carbon disc and Cu plate showed a Co:Ni:Fe ratio of 16:57:27. The sample deposited on Au sputtered AAO had a Co:Ni:Fe ratio of 19:58:23.

Magnetic measurements of prepared CoNiFe nanostructures were performed at room temperature using a VSM. Fig. 6a and b shows the reduced hysteresis curves of the CoNiFe nanotube arrays obtained from the Au sputtered AAO template and the Au sputtered AAO template with stuck conducting carbon disc, respectively. Fig. 6c shows the CoNiFe nanowire arrays on the Au sputtered AAO, with Cu plate and conducting carbon disc. The reduced hysteresis curves show that the magnetic behavior of the CoNiFe nanoarrays is strongly dependent on the template and whether it was sputtered or conductors stuck on to the back side of AAO. The magnetization loops of the CoNiFe nanotube arrays obtained with the Au sputtered AAO template did not reach saturation at 10 kOe. The coercivities of the CoNiFe nanotube arrays obtained on the Au sputtered AAO with stuck conducting carbon disc were 72 Oe and 43 Oe for the applied field perpendicular to and parallel to the nanotube arrays, respectively. Likewise, the coercivites for nanowire arrays deposited on the Au sputtered AAO with stuck conducting carbon disc and Cu plate were 83 Oe and 109 Oe, for the applied field perpendicular to and parallel to the nanowire arrays, respectively (Fig. 6c). Fig. 6b and c shows that the nanowire and nanotube arrays were saturated when the magnetic field was applied along the tube or wire axis with the value of the saturation magnetization at about 5 kOe. That is to say, the easy axis of magnetization of these samples is close to the long axis of the nanotube or nanowire. Results showed that the coercivity values for nanotubes are slightly smaller comparing to nanowire, this could be due to the shape anisotropy effect.

It has been reported that tube formation can be attributed to H_2 generation from the side reactions [22]. It has also been reported that the density of tubes and their shapes is affected by the sputtering time [23]. When the back of the AAO pores is not fully filled by a first sputtering stage, nanowires were not formed and short nanotubes structures were observed. It is necessary to sputter at least 50 nm Au on to the back of the Al_2O_3 for nanowire production. However, this procedure is expensive and takes a long time. Our results indicate that the back electrode is an important factor for controlling the shapes and properties of the nanostructures.

4. Conclusion

CoNiFe nanotubes and nanowires have been successfully electrodeposited on vitreous templates placed on highly ordered porous anodic alumina oxide. It was found that the back electrode placed on AAO template is an important factor in controlling the shapes and properties of the nanostructures. It was observed from SEM micrographs that the nanostructures electrodeposited on Au sputtered AAO are nanotubes, but on Au sputtered AAO with stuck conducting carbon disc and Cu plate are nanowires.

Acknowledgments

This work was supported by TUBITAK with Project number TBAG-105T459 and Inonu University with Project number I.U.A.F-2008/64.

References

[1] B.R. Martin, D.J. Dermody, B.D. Reis, Adv. Mater. 11 (1999) 1021.
[2] L. Piraux, J.M. George, J.F. Despres, Appl. Phys. Lett. 65 (1994) 2484.
[3] C.N.R. Rao, A. Muler, A.A.K. Cheetham, The Chemistry of Nanomaterials, Wiley-VCH, Weinheim, 2004.
[4] Y. Xia, P. Yang, Y. Sun, Y. Wu, B. Mayers, B. Gates, Y. Yin, F. Kim, H. Yan, Adv. Mater. 15 (2003) 353.
[5] S. Dubois, C. Marchal, J.-M. Beuken, L. Piraux, J.-L. Duvail, A. Fert, J.-M. George, J.-L. Maurice, Appl. Phys. Lett. 70 (1997) 396.
[6] A. Blondel, J.P. Meier, B. Doudin, J.P. Ansermet, Appl. Phys. Lett. 65 (1994) 3019.
[7] X. Xu, G. Zangari, J. Appl. Phys. 97 (2005) 10, A3061.
[8] J.L. Duvail, S. Dubois, S. Demoustier-Champagne, Y. Long, L. Piraux, Int. J. Nanotechnol. 5 (2008) 838.
[9] X.P. Li, Z.J. Zhao, S. Ang, T.B. Oh, T.W. Song, W.C. Hg, S.J. Koh, J.Y. Lee, Mater. Sci. Forum 437 (2003) 61.
[10] X.P. Li, Z.J. Zhao, C. Chua, H.L. Seet, L. Lu, J. Appl. Phys. 94 (2003) 6655.
[11] L.P. Liu, Z.J. Zhao, J.C. Zhang, Z.M. Wu, J.Z. Ruan, Q.J. Wang, X.L. Yang, J. Magn. Magn. Mater. 305 (2006) 212.
[12] A.G. Munoz, C. Schiefer, T. Nentwig, J. Phys. D—Appl. Phys. 40 (2007) 5013.
[13] F.E. Atalay, H. Kaya, S. Atalay, Physica B 371 (2006) 327.
[14] F.E. Atalay, H. Kaya, S. Atalay, Mater. Sci. Eng. B 131 (2006) 242.
[15] F.E. Atalay, H. Kaya, S. Atalay, J. Alloys Compd. 420 (2006) 9.
[16] G.V. Kurlyandskaya, J.M. Barandiaran, J.L. Munoz, J. Gutierrez, M. Vazquez, D. Garcia, V.O. Vaskovskiy, J. Appl. Phys. 87 (2000) 4822.
[17] J.P. Sinnecker, M. Knobel, K.R. Pirota, J.M. Garcia, A. Asenjo, M. Vazquez, J. Appl. Phys. 87 (2000) 4825.
[18] F.E. Atalay, S. Atalay, J. Alloys Compd. 392 (2005) 322.
[19] F.E. Atalay, H. Kaya, S. Atalay, J. Phys. D—Appl. Phys. 39 (2006) 431.
[20] R.S. Beach, N. Smith, C.L. Platt, F. Jeffers, A.E. Berkowitz, Appl. Phys. Lett. 68 (1996) 2753.
[21] A.E. Mahdi, L. Panina, D. Mapps, Sens. Actuators A 105 (2003) 271.
[22] Y. Fukunaka, M. Motoyama, Y. Konishi, R. Ishii, Electrochem. Solid-State Lett. 9 (2006) pC62.
[23] D.M. Davis, E.J. Podlaha, Electrochem. Solid-State Lett. 8 (2005) pD1.
[24] M. Motoyama, Y. Fukunaka, T. Saka, Y.H. Ogata, Electrochim. Acta 53 (2007) 205.
[25] H. Cao, L. Wang, Y. Qiu, Q. Wu, G. Wang, L. Zhang, X. Liu, ChemPhysChem 7 (2006) 1500.
[26] F.E. Atalay, M.Sc. thesis, Inonu University, Malatya, Turkey, 1994.
[27] D. Gangasingh, J.B. Talbot, J. Electrochem. Soc. 138 (1991) 3605.
[28] J.M. Quemper, S. Nicolas, J.P. Gilles, J.P. Grandchamp, A. Bosseboeuf, T. Bourouina, E. Dufour-Gergam, Sens. Actuator A 74 (1999) 1.
[29] N. Zech, E.J. Podlaha, D. Landolt, J. Electrochem. Soc. 146 (1999) 2886.
[30] A.G. Munoz, D.R. Salinas, J.B. Bessone, Thin Solid Films 429 (2003) 119.
[31] F.E. Atalay, H. Kaya, S. Atalay, S. Tari, www.sciencedirect.com/dx.doi.org/10.1016/j.jallcom.2008.01.141.